Supporting Information

Cellmer et al. 10.1073/pnas.1019552108

SI Text

The villin headpiece contains 76 residues, which are usually numbered 1–76, with Leu42 being the first residue of the 35-residue C-terminal subdomain. In this work this subdomain is called HP35. Many of the studies, particularly those of Raleigh and coworkers, also include a methionine at the N terminus, which is not present in the naturally occurring sequence, but is present when the polypeptide is synthesized by recombinant methods (1–3). This structure is referred to as HP36, with the methionine labeled residue 41. Here we call this molecule Met-HP35.

Comparison of HP35 Folding Rates from Different Experimental Methods. Table S1 lists published folding rates of HP35 constructs measured from laser temperature-jump (T-jump) experiments with IR and fluorescence detection, triplet-lifetime experiments, and NMR line-shape analysis.

Equilibrium Measurements. Circular dichroism measurements were made with a Jasco 720 spectropolarimeter using 50 μM protein in a 1 mm quartz cuvette. Data were collected at 222 nm. Each measurement was performed at least three times using a different stock solution of protein. The GdmCl concentration was determined by refractometry using an ABBE refractometer (American Optical). The solutions contained 1 mM Tris(2-carboxyethyl) phosphine (TCEP) to prevent disulfide formation, and were buffered to pH = 4.9 with 20 mM sodium acetate. The data were fit with the following equations

$$\Theta_{222\,\mathrm{nm}} = \frac{a + cK_{eq}}{K_{eq} + 1} \qquad K_{eq} = \exp\left\{\frac{m}{RT}([D] - [D_{\mathrm{mid}}])\right\}, \quad \textbf{[S1]}$$

where a is the intercept of the folded baseline, c is the intercept of the unfolded baseline, $\Theta_{222\,\mathrm{nm}}$ is the molar ellipticity at 222 nm, K_{eq} is the equilibrium constant ($=k_u/k_f$), T is the absolute temperature, R is the gas constant, m is the equilibrium sensitivity to denaturant, $[D]$ is the denaturant concentration, and $[D]_{\mathrm{mid}}$ is the denaturant concentration where the population of the folded state is 50%. The fitting parameters a, b, c, m, and $[D]_{\mathrm{mid}}$ were calculated by minimizing the χ^2 parameter

$$\chi^2 = \sum_{i=1}^{N} \frac{(y_{\mathrm{meas}} - y_{\mathrm{calc}})^2}{\sigma_{y_i}^2}. \quad \textbf{[S2]}$$

The weights (σ_y) were set to the standard deviation of at least three measurements. Uncertainties in the resulting fit parameters, m and $[D]_{\mathrm{mid}}$, were calculated by fixing the baseline intercepts to their optimum values and finding parameter values that correspond to a 68% confidence interval. For example, for calculating the uncertainty in m, m was moved from its optimum value and the data refit allowing $[D]_{\mathrm{mid}}$ to vary. The difference between the optimum value of m and that corresponding to the 68% confidence interval is reported as the uncertainty.

Temperature-Jump Measurements. T-jump measurements were carried out on solutions containing 300 μM Cys-HP35(Nle24,His27, Nle29) or N-acetyl-tryptophanamide (NATA) using a nanosecond-laser-temperature-jump instrument very similar to that described in ref. 4. All solutions were buffered to pH = 4.9 with 20 mM sodium acetate and contained 1 mM TCEP to prevent disulfide bond formation, and flowed through the illuminated region to eliminate effects of tryptophan photodamage. Temperature jumps of approximately 5 °C were generated by Raman shifting pulses of a Nd:YAG fundamental at 1,064–1,560 nm using D_2 gas. To ensure a consistent temperature jump in the presence of changing solvent conditions, the temperature jump was calibrated using NATA. A frequency-doubled Kr laser with an output at 284 nm was used to excite Trp fluorescence. In each experiment, four to eight traces of 512 laser shots were collected. Rate constants and amplitudes were calculated by a least-squares fit of the data to a sum of exponentials and baseline from a NATA trace. Fig. S1 plots the measured relaxation times as a function of GdmCl concentration. The uncertainties in the fits were typically much lower than the experiment-to-experiment variation. The uncertainties represent the deviation or the standard deviations from the mean of two to three measurements, respectively, made with different stock solutions and different temperature-jump calibrations. Denaturant concentrations of the samples were calculated using refractometry.

At GdmCl concentrations lower than 2.25 M, the population of unfolded molecules was too small to yield measurable kinetic amplitudes. Thus multiple measurements were made at higher temperatures and the rate at 10 °C was obtained by extrapolation using an Arrhenius expression. Measurements at each temperature were performed three to four times on different days with different temperature-jump calibrations. Solution conditions, other than the GdmCl concentration, and the fitting of the measured traces were the same as reported in *Materials and Methods*. Fig. S4 shows the measured relaxation rates, the folding rates, and the Arrhenius fit of the folding rates. Uncertainties in the relaxation rates are reported as the standard deviation of replicate measurements. Folding rates were calculated from the equilibrium constant and the relaxation rate as discussed in the text. The data were fit to an Arrhenius expression using weighted linear least-squares. The equilibrium constants were obtained by fitting CD data (Fig. S3) as a function of temperature. The following expressions were used to calculate the equilibrium thermodynamic parameters,

$$\Theta_{222\,\mathrm{nm}} = \frac{(a + bT) + (c + dT)K_{eq}}{K_{eq} + 1} \quad \textbf{[S3]}$$

$$K_{eq} = \exp\left\{\frac{\Delta H}{R}\left(\frac{1}{T_f} - \frac{1}{T}\right)\right\}, \quad \textbf{[S4]}$$

where a is the intercept of the folded baseline, b is the slope of the folded baseline, c is the intercept of the unfolded baseline, d is the slope of the unfolded baseline, $\Theta_{222\,\mathrm{nm}}$ is the molar ellipticity at 222 nm, K_{eq} is the equilibrium constant ($=k_u/k_f$), T is the temperature, R is the gas constant, ΔH is the enthalpy difference between the folded and unfolded states, T is the temperature, and T_f is the temperature where the populations of folded and unfolded states are equal.

Triplet-Lifetime Measurements. The population of the tryptophan triplet state was monitored by triplet–triplet absorption at 440 nm using an instrument very similar to that described earlier (5–7). The sample was excited at 290 nm by a 1-mJ pulse from a Ce:LiCaF laser pumped by the fourth harmonic of a Q-switched Nd:YAG laser. The absorbance was probed by monitoring the transmitted intensities of a split 440-nm diode laser beam using

a pair of photodiodes. The measured intensities were averaged over 256 laser shots. A 1.0 cm fluorescence cuvette was used for the absorbance measurements. All samples contained 100 μM Cys-HP35(Nle24,Nle29) in 20 mM sodium acetate buffer with 1 mM TCEP at pH = 4.9. Solutions were deoxygenated and saturated with N_2O to scavenge hydrated electrons produced by tryptophan excitation. Fit parameters are listed in Table S2 and additional traces are found in Fig. S2.

SI Bibliography of Papers on the Villin Headpiece Subdomain

SI Experimental Papers

X-Ray Structures. Chiu TK, Kubelka J, Herbst-Irmer R, Eaton WA, Hofrichter J, Davies DR (2005) High-resolution X-ray crystal structures of the villin headpiece subdomain, an ultrafast folding protein. *Proc Natl Acad Sci USA* 102:7517-7522.

Kubelka J, Chiu TK, Davies DR, Eaton WA, Hofrichter J (2006) Submicrosecond protein-folding. *J Mol Biol* 359:546-553.

NMR and IR Structure and Dynamics. McKnight CJ, Matsudaira PT, Kim PS (1997) NMR structure of the 35-residue villin headpiece subdomain. *Nat Struct Biol* 4:180–184.

Vugmeyster L, Trott O, McKnight CJ, Raleigh DP, Palmer AG (2002) Temperature-dependent dynamics of the villin headpiece helical subdomain, an unusually small thermostable protein. *J Mol Biol* 320:841–854.

Massi F, Palmer AG (2003) Temperature dependence of NMR order parameters and protein dynamics. *J Am Chem Soc* 125:11158–11159.

Wang MH, Tang YF, Sato SS, Vugmeyster L, McKnight CJ, Raleigh DP (2003) Dynamic NMR line-shape analysis demonstrates that the villin headpiece subdomain folds on the microsecond timescale. *J Am Chem Soc* 125:6032–6033.

Tang YF, Rigotti DJ, Fairman R, Raleigh DP (2004) Peptide models provide evidence for significant structure in the denatured state of a rapidly folding protein: The villin headpiece subdomain. *Biochemistry* 43:3264–3272.

Havlin RH, Tycko R (2005) Probing site-specific conformational distributions in protein-folding with solid-state NMR. *Proc Natl Acad Sci USA* 102:3284–3289.

Tang YF, Goger MJ, Raleigh DP (2006) NMR characterization of a peptide model provides evidence for significant structure in the unfolded state of the villin headpiece helical subdomain. *Biochemistry* 45:6940–6946.

Cornilescu G, Hadley EB, Woll MG, Markley JL, Gellman SH, Cornilescu CC (2007) Solution structure of a small protein containing a fluorinated side chain in the core. *Protein Sci* 16:14–19.

Gronwald W, Hohm T, Hoffmann D (2008) Evolutionary Pareto-optimization of stably folding peptides. *BMC Bioinf* 109:9.

Vugmeyster L, McKnight CJ (2008) Slow motions in chicken villin headpiece subdomain probed by cross-correlated NMR relaxation of amide NH bonds in successive residues. *Biophys J* 95:5941–5950.

Thurber KR, Tycko R (2008) Biomolecular solid-state NMR with magic-angle spinning at 25 K. *J Magn Reson* 195:179–186.

Meng WL, Shan B, Tang YF, Raleigh DP (2009) Native-like structure in the unfolded state of the villin headpiece helical subdomain, an ultrafast folding protein. *Protein Sci* 18:1692–1701.

Xiao S, Bi Y, Shan B, Raleigh DP (2009) Analysis of core packing in a cooperatively folded miniature protein: The ultrafast folding villin headpiece helical subdomain. *Biochemistry* 48:4707–4616.

Vugmeyster L (2009) Slow backbone dynamics of chicken villin headpiece subdomain probed by NMR C'-N cross-correlated relaxation. *Magn Reson Chem* 47:746–751.

Hu KN, Havlin RH, Yau WM, Tycko R (2009) Quantitative determination of site-specific conformational distributions in an unfolded protein by solid-state nuclear magnetic resonance. *J Mol Biol* 392:1055–1073.

Bagchi S, Falvo C, Mukamel S, Hochstrasser RM (2009) 2D-IR Experiments and simulations of the coupling between amide-I and ionizable side chains in proteins: Application to the villin headpiece. *J Phys Chem B* 113:11260–11273.

Vugmeyster L, Ostrovsky D, Ford JJ, Lipton AS (2010) Freezing of dynamics of a methyl group in a protein hydrophobic core at cryogenic temperatures by deuteron NMR spectroscopy. *J Am Chem Soc* 132:4038–4039.

Hu KN, Yau WM, Tycko R (2010) Detection of a transient intermediate in a rapid protein-folding process by solid-state nuclear magnetic resonance. *J Am Chem Soc* 132:24–25.

Urbanek, DC, Vorobyev, DY, Serrano, AL, Gai, F, Hochstrasser, RM (2010). The two-dimensional vibrational echo of a nitrile probe of the villin HP35 protein. *J Phys Chem Lett*, 23:3311–3315.

Hu KN, Tycko R (2010) What can solid-state NMR contribute to our understanding of protein folding? *Biophys Chem* 151: 10–21.

Vugmeyster L, Ostrovsky D, Moses M, Ford JJ, Lipton AS, Hoatson GL, Vold RL (2010) Comparative dynamics of leucine methyl groups in FMOC-leucine and in a protein hydrophobic core probed by solid-state deuteron nuclear magnetic resonance over 7–324 K temperature range. *J Phys Chem B* 114: 15799–15807.

Thermodynamics. McKnight CJ, Doering DS, Matsudaira PT, Kim PS (1996) A thermostable 35-residue subdomain within villin headpiece. *J Mol Biol* 260:126–134.

Frank BS, Vardar D, Buckley DA, McKnight CJ (2002) The role of aromatic residues in the hydrophobic core of the villin headpiece subdomain. *Protein Sci* 11:680–687.

Woll MG, Hadley EB, Mecozzi S, Gellman SH (2006) Stabilizing and destabilizing effects of phenylalanine → F-5-phenylalanine mutations on the folding of a small protein. *J Am Chem Soc* 128:15932–15933.

Bi Y, Cho JH, Kim EY, Shan B, Schindelin H, Raleigh DP (2007) Rational design, structural and thermodynamic characterization of a hyperstable variant of the villin headpiece helical subdomain. *Biochemistry* 46:7497–7505.

Gao J, Kelley JW (2008) Toward quantification of protein backbone–backbone hydrogen bonding energies: An energetic analysis of an amide-to-ester mutation in an alpha-helix within a protein. *Protein Sci* 17:1095–1101.

Godoy-Ruiz R, Henry ER, Kubelka J, Hofrichter J, Munoz V, Sanchez-Ruiz JM, Eaton WA (2008) Estimating free-energy barrier heights for an ultrafast folding protein from calorimetric and kinetic data. *J Phys Chem B* 112:5938–5949.

Glasscock JM, Zhu YJ, Chowdhury P, Tang J, Gai F (2008) Using an amino acid fluorescence resonance energy transfer pair to probe protein unfolding: Application to the villin headpiece subdomain and the LysM domain. *Biochemistry* 47:11070–11076.

Zheng TY, Lin YJ, Horng JC (2010) Thermodynamic consequences of incorporating 4-substituted proline derivatives into a small helical protein. *Biochemistry* 49:4255–4263.

Xiao SF, Raleigh DP (2010) A critical assessment of putative gatekeeper interactions in the villin headpiece helical subdomain. *J Mol Biol* 401:274–285.

Goldberg JM, Batjargal S, Petersson EJ (2010) Thioamides as fluorescence quenching probes: Minimalist chromophores to monitor protein dynamics. *J Am Chem Soc* 132:14718–14720.

Kinetics. Hansen KC, Rock RS, Larsen RW, Chan SI (2000) A method for photoinitiating protein folding in a nondenaturing environment. *J Am Chem Soc* 122:11567–11568.

Wang MH, Tang YF, Sato SS, Vugmeyster L, McKnight CJ, Raleigh DP (2003) Dynamic NMR line-shape analysis demonstrates that the villin headpiece subdomain folds on the microsecond timescale. *J Am Chem Soc* 125:6032–6033.

Kubelka J, Eaton WA, Hofrichter J (2003) Experimental tests of villin subdomain folding simulations. *J Mol Biol* 329:625–630.

Buscaglia M, Kubelka J, Eaton WA, Hofrichter J (2005) Determination of ultrafast protein folding rates from loop formation dynamics. *J Mol Biol* 347:657–664.

Brewer SH, Vu DM, Tang YF, Li Y, Franzen S, Raleigh DP, Dyer RB (2005) Effect of modulating unfolded-state structure on the folding kinetics of the villin headpiece subdomain. *Proc Natl Acad Sci USA* 102:16662–16667.

Kubelka J, Chiu TK, Davies DR, Eaton WA, Hofrichter J (2006) Submicrosecond protein folding. *J Mol Biol* 359:546–553.

Brewer SH, Song BB, Raleigh DP, Dyer RB (2007) Residue specific resolution of protein-folding dynamics using isotope-edited infrared temperature-jump spectroscopy. *Biochemistry* 46:3279–3285.

Cellmer T, Henry ER, Kubelka J, Hofrichter J, Eaton WA (2007) Relaxation rate for an ultrafast folding protein is independent of chemical denaturant concentration. *J Am Chem Soc* 129:14564–14565.

Kubelka J, Henry ER, Cellmer T, Hofrichter J, Eaton WA (2008) Chemical, physical, and theoretical kinetics of an ultrafast folding protein. *Proc Natl Acad Sci USA* 105:18655–18662.

Cellmer T, Henry ER, Hofrichter J, Eaton WA (2008) Measuring landscape roughness in ultrafast folding kinetics. *Proc Natl Acad Sci USA* 105:18320–18325.

Bunagan MR, Gao JM, Kelly JW, Gai F (2009) Probing. the folding transition state structure of the villin headpiece subdomain via side chain and backbone mutagenesis. *J Am Chem Soc* 131:7470–7476.

Hu KN, Yau WM, Tycko R (2010) Detection of a transient intermediate in a rapid protein-folding process by solid-state nuclear magnetic resonance. *J Am Chem Soc* 132:24–25.

Reiner A, Henklein P, Kiefhaber T (2010) An unlocking/relocking barrier in conformational fluctuations of villin headpiece subdomain. *Proc Natl Acad Sci USA* 107:4955–4960.

Baldwin RL, Frieden C, Rose GD (2010) Dry molten globule intermediates and the mechanism of protein unfolding. *Proteins: Struct Funct Bioinf* 78:2725–2737.

Other. Bi Y, Tang YF, Raleigh DP, Cho JH (2006) Efficient high level expression of peptides and proteins as fusion proteins with the N-terminal domain of L9: Application to the villin headpiece helical subdomain. *Protein Expression Purif* 47:234–240.

SI Theoretical Papers

Theoretical Models. Islam SA, Karplus M, Weaver DL (2002) Application of the diffusion–collision model to the folding of three-helix bundle proteins. *J Mol Biol* 318:199–215.

Henry ER, Eaton WA (2004) Combinatorial modeling of protein-folding kinetics: Free-energy profiles and rates. *Chem Phys* 307:163–185.

Cellmer T, Henry ER, Kubelka J, Hofrichter J, Eaton WA (2007) Relaxation rate for an ultrafast folding protein is independent of chemical denaturant concentration. *J Am Chem Soc* 129:14564–14565.

Godoy-Ruiz R, Henry ER, Kubelka J, Hofrichter J, Munoz V, Sanchez-Ruiz JM, Eaton WA (2008) Estimating free-energy barrier heights for an ultrafast folding protein from calorimetric and kinetic data. *J Phys Chem B* 112:5938–5949.

Cellmer T, Henry ER, Hofrichter J, Eaton WA (2008) Measuring landscape roughness in ultrafast folding kinetics. *Proc Natl Acad Sci USA* 105:18320–18325.

Computer Simulations: Molecular (Langevin) Dynamics of all Atom Models with Implicit Solvent. Wang JM, Wang W, Huo SH, Lee M, Kollman PA (2001) Solvation model based on weighted solvent accessible surface area. *J Phys Chem B* 105:5055–5067.

Zagrovic B, Snow CD, Khaliq S, Shirts MR, Pande VS (2002) Native-like mean structure in the unfolded ensemble of small proteins. *J Mol Biol* 323:153–164.

Zagrovic B, Pande VS (2003) Structural correspondence between the alpha-helix and the random-flight chain resolves how unfolded proteins can have native-like properties. *Nat Struct Biol* 10:955–961.

He JB, Zhang ZY, Shi YY, Liu HY (2003) Efficiently explore the energy landscape of proteins in molecular dynamics simulations by amplifying collective motions. *J Chem Phys* 119:4005–4017.

Kinnear BS, Jarrold MF, Hansmann UHE (2004) All-atom generalized-ensemble simulations of small proteins. *J Mol Graphics Modell* 22:397–403.

Ripoll DR, Vila JA, Scheraga HA (2004) Folding of the villin headpiece subdomain from random structures. Analysis of the charge distribution as a function of pH. *J Mol Biol* 339:915–925.

Wen EZ, Hsieh MJ, Kollman PA, Luo R (2004) Enhanced ab initio protein-folding simulations in Poisson–Boltzmann molecular dynamics with self-guiding forces. *J Mol Graphics Modell* 22:415–424.

Zagrovic B, Pande VS (2004) How does averaging affect protein structure comparison on the ensemble level? *Biophys J* 87:2240–2246.

Trebst S, Troyer M, Hansmann UHE (2006) Optimized parallel tempering simulations of proteins. *J Chem Phys* 124:174903.

Ding F, Tsao D, Nie HF, Dokholyan NV (2008) Ab initio folding of proteins with all-atom discrete molecular dynamics. *Structure* 16:1010–1018.

Wei YJ, Nadler W, Hansmann UHE (2008) Backbone and side-chain ordering in a small protein. *J Chem Phys* 128:025105.

Chen J, Brooks CL (2008) Implicit modeling of nonpolar solvation for simulating protein folding and conformational transitions. *Phys Chem Chem Phys* 10:471–481.

Computer Simulations: Molecular Dynamics of all Atom Models with Explicit Solvent. Bandyopadhyay S, Chakraborty S, Balasubramanian S, Bagchi B (2005) Sensitivity of polar solvation dynamics to the secondary structures of aqueous proteins and the role of surface exposure of the probe. *J Am Chem Soc* 127:4071–4075.

Bandyopadhyay S, Chakraborty S, Bagchi B (2006) Exploration of the secondary structure specific differential solvation dynamics between the native and molten globule states of the protein HP-36. *J Phys Chem B* 110:20629–20634.

Wickstrom L, Okur A, Song K, Hornak V, Raleigh DP, Simmerling CL (2006) The unfolded state of the villin headpiece helical subdomain: Computational studies of the role of locally stabilized structure. *J Mol Biol* 360:1094–1107.

Zagrovic B, Pande VS (2006) Simulated unfolded-state ensemble and the experimental NMR structures of villin headpiece yield similar wide-angle solution X-ray scattering profiles. *J Am Chem Soc* 128:11742–11743.

Wickstrom L, Bi Y, Hornak V, Raleigh DP, Simmerling C (2007) Reconciling the solution and X-ray structures of the villin headpiece helical subdomain: Molecular dynamics simulations and double mutant cycles reveal a stabilizing cation–pi interaction. *Biochemistry* 46:3624–3634.

Chakraborty S, Bandyopadhyay S (2008) Dynamics of water in the hydration layer of a partially unfolded structure of the protein HP-36. *J Phys Chem B* 112:6500-6507.

Sinha SK, Chakraborty S, Bandyopadhyay S (2008) Thickness of the hydration layer of a protein from molecular dynamics simulation. *J Phys Chem B* 112:8203–8209.

Bagchi S, Falvo C, Mukamel S, Hochstrasser RM (2009) 2D-IR experiments and simulations of the coupling between amide-I and ionizable side chains in proteins: Application to the villin headpiece. *J Phys Chem B* 113:11260–11273.

Yoda T, Sugita Y, Okamoto Y (2010) Hydrophobic core formation and dehydration in protein folding studied by generalized-ensemble simulations. *Biophys J* 99:1637–1644.

Wei HY, Yang LJ, Gao YQ (2010) Mutation of charged residues to neutral ones accelerates urea denaturation of HP-35. *J Phys Chem B* 114:11820–11826.

Computer Simulations: Kinetics and Mechanism of Folding Using Simplified Representations. Srinivas G, Bagchi B (2002) Foldability and the funnel of HP-36 protein sequence: Use of hydropathy scale in protein folding. *J Chem Phys* 116:8579–8587.

Srinivas G, Bagchi B (2002) Folding and unfolding of chicken villin headpiece: Energy landscape of a single-domain model protein. *Curr Sci* 82:179–185.

Sullivan DC, Kuntz ID (2002) Protein folding as biased conformational diffusion. *J Phys Chem B* 106:3255–3262.

Fernandez A, Shen MY, Colubri A, Sosnick TR, Berry RS, Freed KF (2003) Large-scale context in protein folding: Villin headpiece. *Biochemistry* 42:664–671.

Carr JM, Wales DJ (2005) Global optimization and folding pathways of selected alpha-helical proteins. *J Chem Phys* 123:234901.

Knott M, Chan HS (2006) Criteria for downhill protein folding: Calorimetry, chevron plot, kinetic relaxation, and single-molecule radius of gyration in chain models with subdued degrees of cooperativity. *Proteins: Struct Funct Bioinf* 65:373–391.

Senturk S, Baday S, Arkun Y, Erman B (2007) Optimum folding pathways for growing protein chains. *Phys Biol* 4:305–316.

Computer Simulations: Kinetics and Mechanism from Molecular (Langevin) Dynamics of all Atom Models with Implicit Solvent. Shen MY, Freed KF (2002) All-atom fast protein-folding simulations: The villin headpiece. *Proteins: Struct Funct Genet* 49:439–445.

Lei HX, Duan Y (2007) Two-stage folding of HP-35 from ab initio simulations. *J Mol Biol* 370:196–206.

Pande VS, Baker I, Chapman J, Elmer SP, Khaliq S, Larson SM, Rhee YM, Shirts MR, Snow CD, Sorin EJ, Zagrovic B (2003) Atomistic protein-folding simulations on the submillisecond timescale using worldwide distributed computing. *Biopolymers* 68:91–109.

Lei HX, Deng XJ, Wang ZX, Duan Y (2008) The fast-folding HP35 double mutant has a substantially reduced primary folding free-energy barrier. *J Chem Phys* 129:155104.

Lee IH, Kim SY, Lee J (2010) Dynamic folding pathway models of the villin headpiece subdomain (HP-36) structure. *J Comput Chem* 31:57–65.

Lei HX, Su Y, Jin LA, Duan Y (2010) Folding network of villin headpiece subdomain. *Biophys J* 99:3374–3384.

Computer Simulations: Kinetics and Mechanism from Molecular Dynamics of all Atom Models with Explicit Solvent. Duan Y, Kollman PA (1998) Pathways to a protein folding intermediate observed in a 1-microsecond simulation in aqueous solution. *Science* 282:740–744.

Duan Y, Wang L, Kollman PA (1998) The early stage of folding of villin headpiece subdomain observed in a 200-nanosecond fully solvated molecular dynamics simulation. *Proc Natl Acad Sci USA* 95:9897–9902.

Lee MR, Duan Y, Kollman PA (2000) Use of MM-PB/SA in estimating the free energies of proteins: Application to native, intermediates, and unfolded villin headpiece. *Proteins: Struct Funct Genet* 39:309–316.

Sullivan DC, Kuntz ID (2001) Conformation spaces of proteins. *Proteins: Struct Funct Genet* 42:495–511.

Jang SM, Kim E, Shin S, Pak Y (2003) Ab initio folding of helix bundle proteins using molecular dynamics simulations. *J Am Chem Soc* 125:14841–14846.

De Mori GMS, Micheletti C, Colombo G (2004) All-atom folding simulations of the villin headpiece from stochastically selected coarse-grained structures. *J Phys Chem B* 108: 12267–12270.

De Mori GMS, Colombo G, Micheletti C (2005) Study of the villin headpiece folding dynamics by combining coarse-grained Monte Carlo evolution and all-atom molecular dynamics. *Proteins: Struct Funct Bioinf* 58:459–471.

Bandyopadhyay S, Chakraborty S, Bagchi B (2006) Coupling between hydration layer dynamics and unfolding kinetics of HP-36. *J Chem Phys* 125:084912.

Jayachandran G, Vishal V, Pande VS (2006) Using massively parallel simulation and Markovian models to study protein folding: Examining the dynamics of the villin headpiece. *J Chem Phys* 124:164902.

Ensign DL, Kasson PM, Pande VS (2007) Heterogeneity even at the speed limit of folding: Large-scale molecular dynamics study of a fast-folding variant of the villin headpiece. *J Mol Biol* 374:806–816.

Hinrichs NS, Pande VS (2007) Calculation of the distribution of eigenvalues and eigenvectors in Markovian state models for molecular dynamics. *J Chem Phys* 126:244101.

Jayachandran G, Vishal V, Garcia AE, Pande VS (2007) Local structure formation in simulations of two small proteins. *J Struct Biol* 157:491–499.

Lucent D, Vishal V, Pande VS (2007) Protein folding under confinement: A role for solvent. *Proc Natl Acad Sci USA* 104:10430–10434.

Sonavane UB, Ramadugu SK, Joshi RR (2008) Study of early events in the protein folding of villin headpiece using molecular dynamics simulation. *J Biomol Struct Dyn* 26:203–214.

Freddolino PL, Schulten K (2009) Common structural transitions in explicit-solvent simulations of villin headpiece folding. *Biophys J* 97:2338–2347.

Bowman GR, Beauchamp KA, Boxer G, Pande VS (2009) Progress and challenges in the automated construction of Markov state models for full protein systems. *J Chem Phys* 131:124101.

Bowman GR, Pande VS (2010) Protein folded states are kinetic hubs. *Proc Natl Acad Sci USA* 107:10890–10895.

Chiang TH, Hsu D, Latombe JC (2010) Markov dynamic models for long-timescale protein motion. *Bioinformatics* 26: i269–i277.

Rajan A, Freddolino PL, Schulten K (2010) Going beyond clustering in MD trajectory analysis: An application to villin headpiece folding. *PLoS One* 5:e9890.

Sinha SK, Chakraborty S, Bandyopadhyay S (2010) Secondary structure specific entropy change of a partially unfolded protein molecule. *Langmuir* 26:9911–9916.

Jain A, Hegger R, Stock G (2010) Hidden complexity of protein free-energy landscapes revealed by principal component analysis by parts. *J Phys Chem Lett* 1:2769–2773.

Freddolino PL, Harrison CB, Liu YX, Schulten K (2010) Challenges in protein-folding simulations. *Nat Phys* 6:751–758.

1. Brewer SH, Song BB, Raleigh DP, Dyer RB (2007) Residue specific resolution of protein-folding dynamics using isotope-edited infrared temperature-jump spectroscopy. *Biochemistry* 46:3279–3285.

2. Brewer SH, Vu DM, Tang YF, Li Y, Franzen S, Raleigh DP, Dyer RB (2005) Effect of modulating unfolded-state structure on the folding kinetics of the villin headpiece subdomain. *Proc Natl Acad Sci USA* 102:16662–16667.

3. Wang MH, Tang YF, Sato SS, Vugmeyster L, McKnight CJ, Raleigh DP (2003) Dynamic NMR line-shape analysis demonstrates that the villin headpiece subdomain folds on the microsecond timescale. *J Amer Chem Soc* 125:6032–6033.
4. Thompson PA, Eaton WA, Hofrichter J (1997) Laser temperature-jump study of the helix reversible arrow coil kinetics of an alanine peptide interpreted with a "kinetic zipper" model. *Biochemistry* 36:9200–9210.
5. Lapidus LJ, Eaton WA, Hofrichter J (2000) Measuring the rate of intramolecular contact formation in polypeptides. *Proc Natl Acad Sci USA* 97:7220–7225.
6. Lapidus LJ, Eaton WA, Hofrichter J (2002) Measuring dynamic flexibility of the coil state of a helix-forming peptide. *J Mol Biol* 319:19–25.
7. Lapidus LJ, Steinbach PJ, Eaton WA, Szabo A, Hofrichter J (2002) Effects of chain stiffness on the dynamics of loop formation in polypeptides. Appendix: Testing a 1-dimensional diffusion model for peptide dynamics. *J Phys Chem B* 106:11628–11640.
8. Buscaglia M, Kubelka J, Eaton WA, Hofrichter J (2005) Determination of ultrafast protein folding rates from loop formation dynamics. *J Mol Biol* 347:657–664.
9. Kubelka J, Eaton WA, Hofrichter J (2003) Experimental tests of villin subdomain folding simulations. *J Mol Biol* 329:625–630.
10. Bunagan MR, Gao JM, Kelly JW, Gai F (2009) Probing. the folding transition state structure of the villin headpiece subdomain via side-chain and backbone mutagenesis. *J Amer Chem Soc* 131:7470–7476.

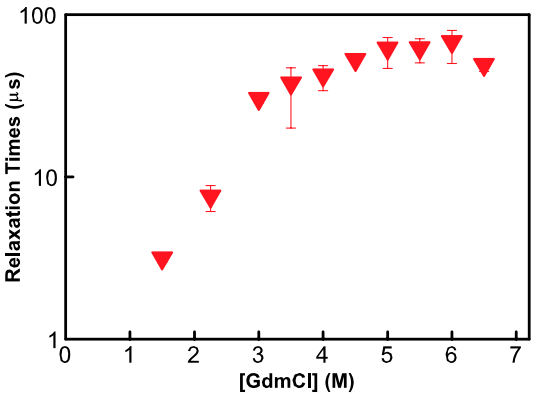

Fig. S1. Cys-HP35(Nle24,His27,Nle29) relaxation times as a function of [GdmCl]. These are the measured relaxation times from temperature-jump experiments, and were used to calculate the folding times in Fig. 7 assuming a two-state model. Further details regarding the experiments are provided in the *SI Text* and in the caption for Fig. 7 in the main text.

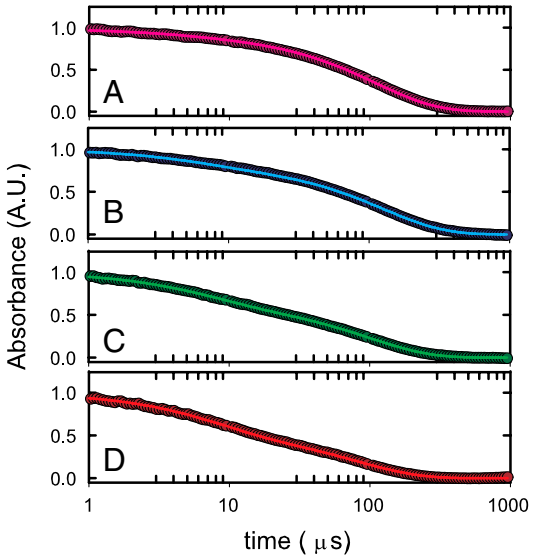

Fig. S2. Triplet-lifetime decays not shown in main text. Normalized tryptophan triplet–triplet absorbance at 440 nm as a function of time on a log scale at 10 °C for 100 μM solutions of Cys-HP35(Nle24,Nle29) containing 20 mM sodium acetate, 1 mM TCEP, and either (*A*) 1.5 M GdmCl (purple), (*B*) 3 M GdmCl (blue), (*C*) 3.5 M GdmCl (green), (*D*) 4.0 M GdmCl (yellow), (*E*) 5.0 M GdmCl (orange), or (*F*) 5.5 M GdmCl (red). The circles are the experimental data and the lines are the fits with the kinetic model.

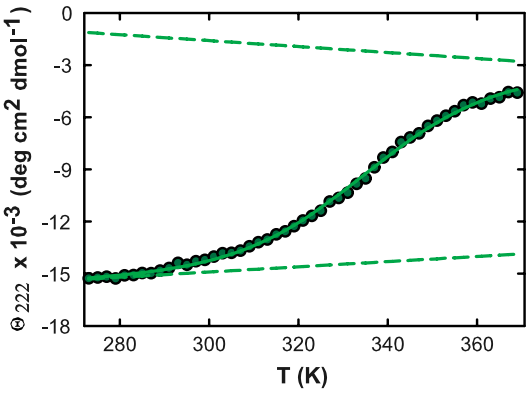

Fig. S3. Equilibrium thermal unfolding curves for 75 μm Cys-HP35(Nle24,His27,Nle29) in 1.5 M GdmCl measured by circular dichroism. The continuous green line represents a two-state fit to the data. The dashed lines are the folded and unfolded baselines used in the calculation of the fraction of folded as a function of temperature. The fitted parameters are $\Delta H_m = 15$ kcal/mol, $T_m = 340$ K, $a = -19.4$ deg cm^2 dmol^{-1}, $b = 0.0149$ deg cm^2 dmol^{-1} K^{-1}, $c = 3.54$ deg cm^2 dmol^{-1}, and $d = -0.0171$ deg cm^2 dmol^{-1} K^{-1}.

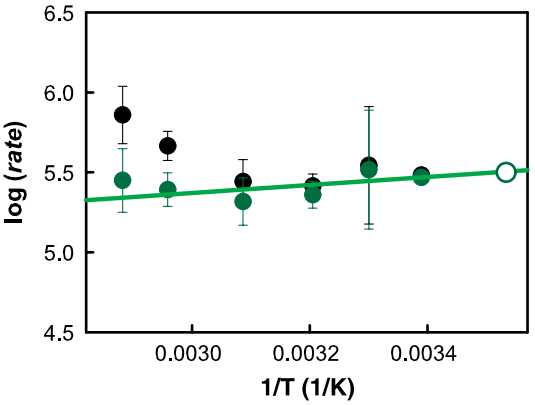

Fig. S4. T-jump kinetics for Cys-HP35(Nle24,His27,Nle29) in 1.5 M GdmCl. Relaxation rates (black circles), folding rates (green circles), and Arrhenius fit (green line) to the folding rates for measurements made at 10 °C in 1.5 M GdmCl, 20 mM sodium acetate, 1 mm TCEP, and pH = 4.9. Using the Arrhenius fit, the data were extrapolated to 283 K, the temperature of the experiments performed in the main text. This point is represented on the plot by the open circle ($k_f = 3.2 \times 10^6$ s^{-1}). The Arrhenius parameters are $T_0 = 300$ K, $k_0 = 2.8 \times 10^6$ s^{-1}, and $\Delta H^* = -1,150$ cal/mol.

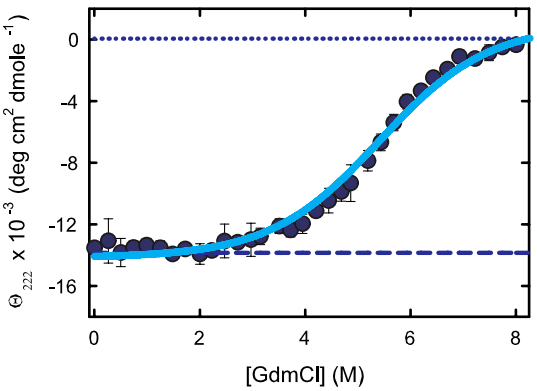

Fig. S5. Fit of triplet-lifetime model to circular dichroism data in simultaneous fit to equilibrium and kinetic data (Fig. 4 and Fig. 7). See *Materials and Methods* for details.

Table S1. Summary of kinetics for HP35 from previous work

Construct	Method	[GdmCl] M	T K	Relaxation time, μs	τ_f, μs	τ_u, μs	τ_f/τ_u	Ref.
Cys-HP-35	triplet lifetime	2.5	303	20 (+6,−4)	31 (+12,−8)	56 (+21,−14)	0.56	(8)*
HP35(His27)	T-jump fluorescence	2.5	303	13.0 (±0.3)	21.0 (±0.7)	37 (±1)	0.56	(8)*
Cys-HP-35	triplet lifetime	2.5	313	22 (+13,−6)	50 (+41,−18)	38 (+33,−14)	1.3	(8)*
HP35(His27)	T-jump fluorescence	2.5	313	7.9(±0.3)	18.0 (±0.9)	14 (±0.7)	1.3	(8)*
HP35(His27)	T-jump fluorescence	0	318	4.4 (±1.0)	4.7 (±1.0)	65 (±13)	0.07	(9)†
HP35(His27)	T-jump infrared	0	318	7.4	8.6	57	0.15	(10)‡
Met-HP35	T-jump infrared	0	318	4.8	—	—	—	(1)§
HP35(His27)	T-jump fluorescence	0	323	4.2 (±0.4)	4.8 (±0.5)	36 (±3)	0.13	(9)†
HP35(His27)	T-jump infrared	0	323	5.6	7.4	31	0.24	(10)‡
Met-HP35	T-jump infrared	0	323	2.3	3.3	7.0	0.47	(2)¶
Met-HP35	NMR	0	341	5.2 (±0.7)	12 (±2)	9.2 (±1.9)	1.3	(3)
HP35	T-jump infrared	0	341	3.0	7.0	5.1	1.4	(10)‡
HP35(His27)	T-jump fluorescence	0	342	2.1 (±0.3)	4.9 (±0.7)	3.6 (±0.5)	1.4	(9)†

Calculated assuming a two-state model.
*0.1 M sodium acetate, pH = 4.8.
†0.02 M sodium acetate, pH = 4.9.
‡0.02 M 2-(*N*-morpholino)ethanesulfonic acid in D_2O, pH = 5.5.
§Obtained from the buried Ala16 labeled with $^{13}C^{18}O$.
¶0.01 M sodium phosphate in D_2O, 0.15 M NaCl, pH = 5.3.

Table S2. Summary of parameters from triplet-quenching measurements

GdmCl [M]	$\log[k_u(s^{-1})]$	$\log[k_q(s^{-1})]$	$\log[k_s(s^{-1})]$	$\log[k_f(s^{-1})]$	$\log(\Lambda_+)$	$\log(\Lambda_-)$	a
1.5	4.04	5.36	3.88	5.68	5.87	4.06	0.002
2.25	3.69	5.32	3.86	5.01	5.47	4.02	0.02
3	3.37	5.27	3.85	4.38	5.33	3.96	0.08
3.5	3.59	5.24	3.83	4.39	5.31	4.01	0.11
4	3.70	5.20	3.82	4.29	5.27	4.05	0.17
4.5	3.67	5.16	3.80	4.05	5.21	4.02	0.26
5	3.65	5.12	3.77	3.82	5.16	4.00	0.37
5.5	3.84	5.07	3.75	3.80	5.12	4.08	0.47
6	3.90	5.02	3.72	3.66	5.06	4.10	0.59

The unfolding rate is k_u, k_q is the quenching rate in the unfolded state, k_s is the quenching rate in the folded state, k_f is the folding rate, Λ_+ is the fast eigenvalue, Λ_- is the slow eigenvalue, and *a* is the fast amplitude (the slow amplitude is 1-*a*).